SIMULATION OF THE APPLICATION ON WAVELET FILTER IN STATIC SYNCHRONOUS COMPENSATOR

[1]REN GUOCAN, [2]WANG SONGLIANG, [3]SHAO HUA

[1]Ningbo City College of Vocational Technology

ABSTRACT

Reactive power balance of power system is important. Static synchronous compensator (STATCOM) based on invert technology is a new dynamic reactive power compensation, and has many advantages compared with static var compensator, so STATCOM has vast market prospect. New technology can improve the performance of static synchronous compensator, and in this paper wavelet filter is applied in STATCOM to filter the harmonics of load current, and the active portion and reactive portion of the fundamental current are calculated by dq transformer, and the reference signal of output current is calculated by dq reverse transformer using the reactive portion and the output of PI controller which controls the DC voltage，and PWM tracking control technology is employed. The simulation results indicate that the application effect is good.

Keywords: *Wavelet Filter, Reactive Power Compensation, STATCOM, Simulation*

1. INTRODUCTION

Reactive power in power grid is the basic reason of the deviation power system voltage from the nominal value. When the voltage deviation gets big, the electrical equipment performance would be deteriorated, which may not only lead to the low operating efficiency of equipment，but also the damage caused by the overvoltage or over current. Big voltage deviation is the thread to the power system's stability and influences the system's economical operation. It's the necessary and sufficient way to ensure every node voltage of power system in normal levels that the power system has plenty of reactive power sources and essential voltage regulation method is used. The SVC and STATCOM have dynamic reactive compensation properties in many kinds of reactive power sources. Compared with SVC, the STATCOM has many superior performances, such as fast governing speed, wide running range, and can greatly reduce the harmonics in the current compensation when the PWM control technique and so on are used. Besides, both the bulk and the weight of the device are decreased because the reactor and capacitor used in STATCOM are far smaller than these in SVC.

Japan and the USA respectively developed a set of 80Mvar and 100Mvar STATCOM device adopted GTO thruster in 1991 and 1994. Both the devices were successfully put into commercial operation. [1]The STATCOM device, of which unit capacity is 8Mvar, was also put into operation in 1998 made by Siemens of Germany. In China, the STATCOM device of ±20 Mvar was run in Chaoyan transformer substation of Henan Power Company in 1999, and in 2005 the STATCOM device of ±50Mvar was installed in Huangdu Xijiao transformer substation, which was used to improve the voltage stability of 220 kV bus and inhibit the bus voltage surge. [2-3]

In this paper, the wavelet filtering is applied in STATCOM, which filters the harmonics in voltage and current, and gets the fundamental voltage and current. Simultaneously, the active portion and reactive portion of the fundamental current are calculated by dq transformer, and the tracking control technology is employed to control the output current of STATCOM, using reactive portion of the fundamental current as reference signal. The output current tracks the reference signal and the source current don't contain fundamental reactive current.

2. THE STATCOM STRUCTURE & WORK PRINCIPLE

The schematic diagram of STATCOM adopted voltage source inverting circuit is shown as Fig 1.The voltage source inverting circuit gets into the power grid through the transformer, which can match the source voltage with the grid voltage. If there is no need to match the two voltages, the inverting circuit can also get into the grid through

the inductance. In order to achieve dynamic reactive power compensation, the output voltage phase and amplitude of the AC-side of convert circuit can be controlled (or directly control the current of AC-side) to make the fundamental reactive current (i_{ac}), which is in the converter circuit, equal with the load fundamental reactive current (i_{al}), and there is no fundamental reactive current in the source current (i_{as}). More thyristors used in series can improve the STATCOM capacity and the voltage grade, which can also be achieved through the multiple technology and multi-level technology.
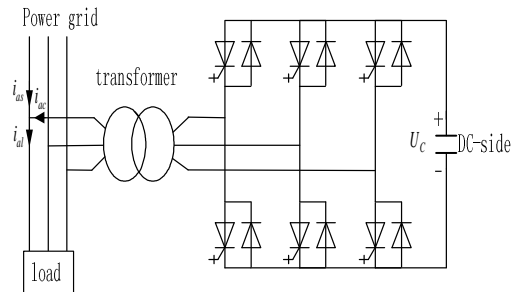

Fig 1. The STATCOM With Voltage Converter Circuit

3. THE THEORY OF WAVELET FILTER

The formula of f (t) ∈ L2(R) is launched following the space combination shown as formula 1, [4-5]

$$L^2(R) = \sum_{j=-\infty}^{J} W_j \oplus V_J$$

（1）

Where J is an arbitrary scale. So, the $f(t)$ can be written as

$$f(t) = \sum_{j=-\infty}^{J} \sum_{k=-\infty}^{\infty} d_{j,k} \psi_{j,k}(t) + \sum_{k=-\infty}^{\infty} c_{j,k} \phi_{j,k}(t)$$

(2)

The signal $f(t)$ is decomposed by 5-layer orthogonal wavelet shown as fig 2.

If the signal fundamental frequency is 50Hz, according to Shannon's sampling theorem, the fundamental signal sampled 128 points per cycle can be analyzed to 64 harmonics (3200Hz). If the maximum frequency of $f(t)$ is 3200Hz, according to Fig 2, the band division on the wavelet decomposition is shown in Table 1, [1] where each decomposition of the signal or low frequency (ca) of the band is down into some low-frequency band (ca) and high frequency band

portion (cd), and the decomposition of the band is in accordance with the highest frequency that can be analyzed. The 128-point sampling is according to the band decomposition at the maximum frequency of 3200Hz. In Table 1, the voltage signal and current signal are 5-layer wavelet decomposition. If the voltage and current without DC and second harmonic, their low frequency (ca5) only contains base wave after the 5 layers of wavelet decomposition.
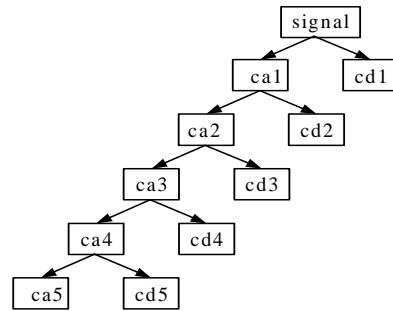

Fig 2. The Wavelet Decomposition

Table 1. The Frequency Band And Harmonics

Wavelet	Frequency band	Harmonics
cd1	1600Hz-3200Hz	32-64
cd2	800Hz-1600Hz	16-32
cd3	400Hz-800Hz	8-16
cd4	200Hz-400Hz	4-8
cd5	100Hz-200Hz	2-4

4. CONTROL OF STATCOM

Block diagram of fundamental reactive load current's detection and power grid reference current's generation is shown in Fig 3,where sine and cosine signal (sinωt, cosωt) are obtained, which have the same frequency and power with the power grid by pll. i_{al}, i_{bl} and i_{cl} are the load current, and the fundamental current (i_{af}, i_{bf} i_{cf}) can be get after wavelet filtering described in step 2. The three-phase fundamental current is assumed as follows,

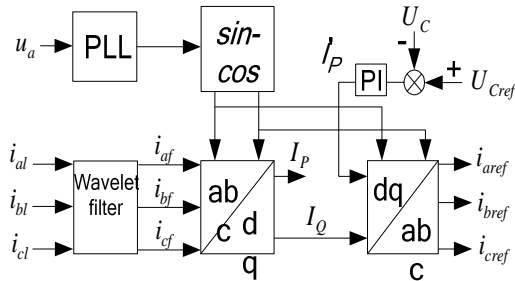*Fig 3. Block Diagram Of The Power Grid Reference Current's Generation*

$$i_{af} = I_m \sin(\omega t - \varphi) \tag{3}$$

$$i_{bf} = I_m \sin(\omega t - 2\pi/3 - \varphi) \tag{4}$$

$$i_{cf} = I_m \sin(\omega t + 2\pi/3 - \varphi) \tag{5}$$

The dq transformer of three-phase current is shown as follows, [1、6] so that the load fundamental current active component and reactive component can be obtained. In order to maintain the DC bus voltage (U_C) stable, closed-loop control of capacitor voltage is used; whose controller is the PI regulator. I_P' Is assumed as the output of PI regulator,

$$
\begin{bmatrix} I_P \\ I_Q \end{bmatrix} = \frac{2}{3}
\begin{bmatrix}
\sin\omega t & \sin(\omega t - \frac{2}{3}\pi) & \sin(\omega t + \frac{2}{3}\pi) \\
\cos\omega t & \cos(\omega t - \frac{2}{3}\pi) & \cos(\omega t + \frac{2}{3}\pi)
\end{bmatrix}
\begin{bmatrix}
I_m \sin(\omega t - \varphi) \\
I_m \sin(\omega t - \frac{2}{3}\pi - \varphi) \\
I_m \sin(\omega t + \frac{2}{3}\pi - \varphi)
\end{bmatrix} =
\begin{bmatrix} I_m \cos\varphi \\ I_m \sin\varphi \end{bmatrix} \tag{6}
$$

The reference signals (i_{aref}、i_{bref} and i_{cref}) of current tracking controlling can be obtained through the dq inverse transformation. The value of d in dq inverse transformation is the PI regulator output I_P', while the value of q is the reactive component (I_Q) of load current. Both of them are shown as follows.

$$
\begin{bmatrix} i_{aref} \\ i_{bref} \\ i_{cref} \end{bmatrix} =
\begin{bmatrix}
\sin\omega t & \cos\omega t \\
\sin(\omega t - \frac{2}{3}\pi) & \cos(\omega t - \frac{2}{3}\pi) \\
\sin(\omega t + \frac{2}{3}\pi) & \cos(\omega t + \frac{2}{3}\pi)
\end{bmatrix}
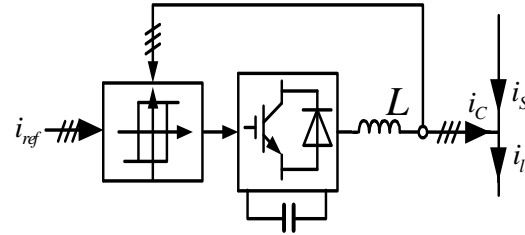\begin{bmatrix} I_P' \\ I_Q \end{bmatrix} \tag{7}
$$

Fig 4. Tracking Control

The output current can be controlled in inverter circuit with PWM Tracking Control Technology. Its working principle is shown in Fig 4, where the reference signal i_{ref} (i_{aref}、i_{bref} and i_{cref}) can make the output compensation current of inverter circuit have the same value 、 phase and frequency with the load fundamental reactive current ,and there is no fundamental reactive current in power current.

5. THE SIMULATION

The power supply system with STATCOM is shown as Fig 5, where the three-phase power is symmetrical. The STATCOM and its control circuit are at the right part of the figure. At the left part, there are access point detection of voltage and current, the three-phase power and its load which is the three-phase full-controlled bridge rectifier circuit. The three-phase power supply is joined by the star-connecting and the equivalent inductance of the power is LS， while the equivalent resistance is not drawn. The current whose characteristic harmonic is 6k±1 (k=1, 2, 3,…), causing the supply point voltage distortion formed by the three-phase full-controlled bridge rectifier circuit. The STATCOM is the three-phase bridge voltage inverter circuit. It is connected to the access point through the inductor LC, whose effect is filtering. The three-phase voltage inverter circuit is controlled using the hysteresis current tracking control technology.

The simulation system is to maintain DC voltage (voltage across the capacitor) of STATCOM stable and compensate the load fundamental reactive current. The grid voltage and load current contain harmonics, which can be filtered by wavelet transform. The signal is decomposed by 5-layer orthogonal wavelet, and the low frequency part (ca5) is reconstructed. According to the frequency division of wavelet decomposition in table.1, the lowest harmonic frequency in the signal is 5, and the reconstruction signal of the low frequency part is just the fundamental signal. So, the lowest harmonic of the voltage and current in the

simulation system is 5 and both the voltage and current are decomposed by 5-lay wavelet, and the fundamental voltage and current can be obtained by the low frequency part's reconstruction.

The simulation results are shown in Fig 6、7、8 and 9. In the 4 figures, the control angle of the full-controlled rectifier bridge has been changed from 5° to 60° at 0.4s. Figure 6 shows the three-phase voltage (uap, ubp, ucp) of the public power supply point (PCC) and its wavelet filtered voltage (ual, ubl, ucl). Figure 7 shows the three-phase load current (ial, ibl, icl) and its wavelet filtered current (iaf, ibf, icf). These two figures indicate that the filter works well. Figure 8 shows the three-phase command current of STATCOM (iaref, ibref, icref) and its actual output three-phase current (iac, ibc, icc). Figure 9 shows the waveforms of three-phase supply voltage (uas, ubs, ucs) and current (ias, ibs, ics).Before 0.4s, the fundamental reactive current is very small, so it is the current generated by STATCOM. The supply current almost has no change compared with the load current. After 0.4s, both the fundamental reactive current and the current generated by STATCOM are big, and the supply current has great changes compared with the load current.
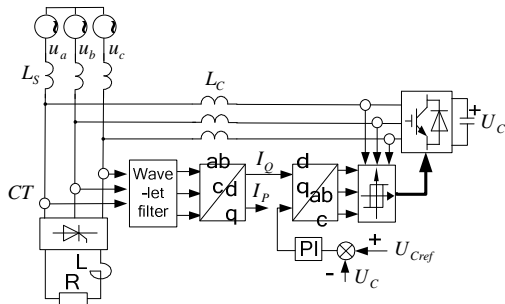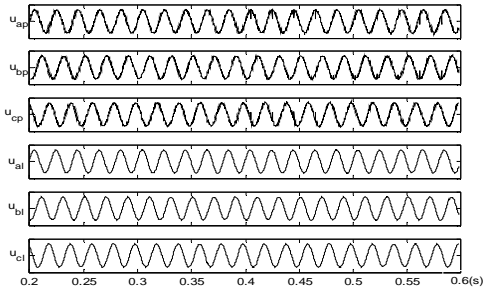

Fig 5. The Power Supply System With STATCOM

Fig 6. The Voltage Of The Public Power Supply Point (PCC) Before And After The Filtering
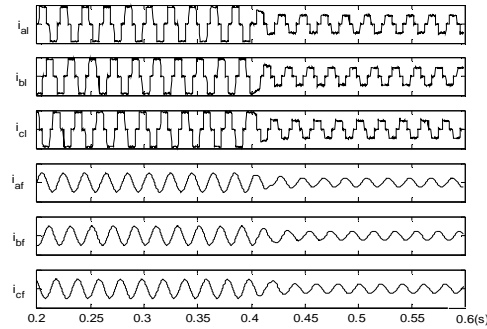

Fig 7. The Current Of The Load Before And After The Filtering

A-frame;   B1-B4-   spring   leaf; C-wave-guide-bridge; M-mass block

The axial elastic coefficient of the two-wave-guide-bridge is

$$K_w = \frac{Ebh}{l}$$

(8)

where E is equivalent elastic modulus of cladding and core of waveguide material; b is width of waveguide bridge; h is thickness of waveguide bridge; l is length of waveguide bridge.
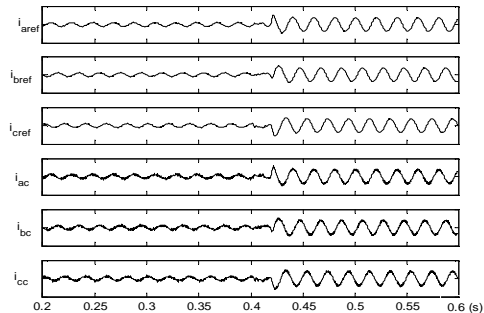

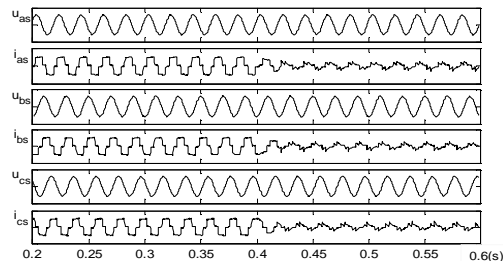*Fig 8. The Command Current And Its Actual Output Current*

Fig 9. The Voltage And Current Of The Source

The elastic coefficient of the four spring leaves is

$$K_p = \hat{E}b'(\frac{h'}{l'})^3 \tag{9}$$

Where $\hat{E}$ is elastic modulus of spring leaf; b' is width of spring leaf; h' is thickness of spring leaf; l' is length of spring leaf.

The resonant frequency of mass-spring system of measuring probe is expressed as

$$f_0 = \frac{1}{2\pi}\sqrt{\frac{K_y}{m}}, \quad K_y = 2K_w + 4K_P \tag{10}$$

The resonant frequencies of spring leaf is expressed as

$$f_{0P} = K_p\sqrt{\frac{\hat{E}}{\rho}}\frac{h'}{l'} \tag{11}$$

While, the resonant frequencies of wave-guide-bridge is expressed as

$$f_{0w} = f_{op}\sqrt{1 + K_w\frac{Nl^2}{Ebh^3}} \tag{12}$$

When wave-guide-bridge generate a uniform dynamic stress, the stress on FBG is associated with acceleration, expressed as

$$\varepsilon_Z = a\frac{m}{K_y l_w} \tag{13}$$

where ε_Z is axial stress of FBG; a is vibration acceleration; m is quality of mass block; l_w is length of FBG.

FBG 1 and FBG 2 are two fibers Bragg gratings which have same center reflected wavelength and are both λ_{b1} with no vibration signals. The reflectance spectrum is shown in Fig.10 (a).

When vibration action is on mass block which is to act on wave-guide-bridge, grid pitch of fiber gratings on Waveguide Bridge is to be changed under uniform stress as shown in Fig.10 (b). And the result in change of reflected wavelength of fiber gratings is $\Delta\lambda_{b11}$. Suppose that compressive stress is generated on FBG 1 and tensile stress on FBG 2 corresponded regularly. Then, wavelengths change of FBG 1 and FBG 2 are expressed respectively as

$$\Delta\lambda_1 = \lambda_{b11} - \lambda_{b1}$$
$$= \lambda_{b1}\{1 - \frac{n_{neff}^2}{2}[(1-\mu)P_{12} - \mu P_{11}]\}(-\varepsilon_Z) + \lambda_{b1}\alpha\Delta T \tag{14}$$

$$\Delta\lambda_2 = \lambda_{b11}' - \lambda_{b1}$$
$$= \lambda_{b1}\{1 - \frac{n_{neff}^2}{2}[(1-\mu)P_{12} - \mu P_{11}]\}\varepsilon_Z + \lambda_{b1}\alpha\Delta T \tag{15}$$

where is lateral Poisson ratio; P_{11}, P_{12} are the Pockel's coefficients of the stress-optic tensor; ε_Z is axial stress (i.e., it's "+" when compressive stress is applied and per contra "-"); α is the coefficient of thermal expansion; ΔT is the temperature difference. Suppose the reflected wavelength difference of FBG 1 and FBG 2 is $\Delta\lambda$, it can be expressed as
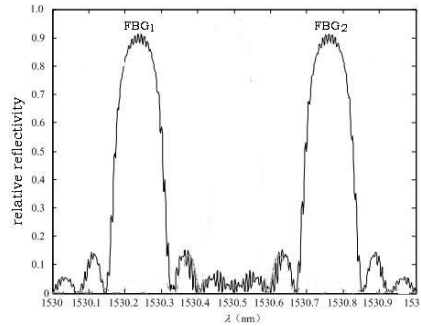
$$\Delta\lambda_{b11} = \Delta\lambda_2 - \Delta\lambda_1 = \lambda_{b1}\{1 - \frac{n_{neff}^2}{2}[(1-\mu)P_{12} - \mu P_{11}]\}\varepsilon_Z \tag{16}$$

Given $K = 1 - \frac{n_{eff}^2}{2}[(1-\mu)P_{12} - \mu P_{11}]$, then

$$\Delta\lambda = 2K\lambda_{b1}\varepsilon_z, \tag{17}$$
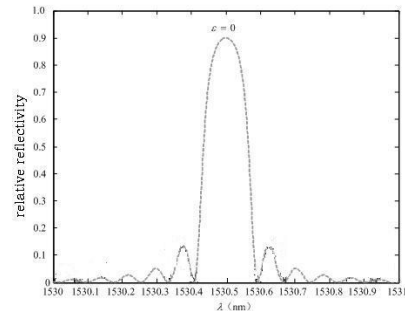
(a)

(b)

Fig 10.Reflectance spectrum of measuring acceleration probe: (a) No strain is applied to FBG1 and FBG2. (b) Strain is applied to FBG1 and FBG2.

Expression (15) indicates that the reflected wavelength difference of FBG$_1$ and FBG$_2$, $\Delta\lambda$ is independent of temperature. In the light of expression (15), we can establish the relationship of wavelength difference $\Delta\lambda$ and vibration acceleration a.

6.   SIMULATION RESULTS

In this section two simulations are carried out for evaluating the performance of the FWNN with the proposed initialization procedure.

Example.1. In order to compare with other research the second order nonlinear dynamic plant in [18] is considered.

$$y(k) = f(y(k-1), y(k-2), y(k-3), u(k), u(k-1)) \qquad (18)$$

In that

$$f(x_1, x_2, x_3, x_4, x_5) = \frac{x_1 x_2 x_3 x_5 (x_3 - 1) + x_4}{1 + x_3^2 + x_2^2} \qquad (19)$$

$y(k-1)$, $y(k-2)$, $y(k-3)$ Are   one, two and

Tree step delayed outputs of the plant are $u(k-1)$ current and one step delayed inputs of the plant. The current output of the plant depends on previous input and output signals. Here same as [18] only the current state of system and the control signal are fed into the FWNN as inputs.

The network is trained for 200 epochs with 1000 time steps in each epoch. The root-mean-square error (RMSE) used as a performance index is as follows where K is the number of training data which is distributed uniformly in [-1, 1] (here K=1000).

$$RMSE = \sqrt{\frac{\sum_{i=1}^{K}(y(k+1) - y_d(k+1))^2}{K}} \qquad (20)$$

The clustering algorithm described in section III.A is used to determine the number of fuzzy rules and the initial parameters of the wavelets. By using that algorithm we construct the FWNN in section II with only two fuzzy rules. The number of parameters is reduced to N=18 and the RMSE obtained after training is 0.003

7.CONCLUSIONS

With the development of microelectronics technology, The DFACTS device, based on full-controlled devices and inverter technology, has been continuously improving its reliability and reducing its ongoing cost. So this device, such as STATCOM 、 APF, has broad application prospects. The wavelet filtering was applied in STATCOM while its simulation was done. The simulation results show that the application works well.

REFERENCE

[1] LIU Wen-hua ， SONG Qiang ， ZHANG Dong-jiang, etc. Equivalent Tests of Links of 50 MVA STATCOM [J]. Proceedings of the CSEE, 2006, 26(12):73-77.

[2] ZHENG Dong-run, QIAO Wei-dong, LIU W en-hua, etc. Field tests of 500Mvar STATCOM [J]. EastChinaElectric Power, 2007, 35(1):47-50.

[3] Weon-Ki Yoon, etc. Reactive Power Measurement Using the Wavelet Transform [J]. IEEE Transactions on Instrumentation and Measurement (S0018-9456), 2000, 49(2): 246-252.

[4] Reactive Power Measurement by Wavelet Transform and Hilbert Transform [J]. JOURNAL OF SYSTEM SIMULATION, 2005, 17(4):822-824.

[5] Li Z.Q., Zheng S.S., Hu Y., Tao Q.G., He W, Failure Modes-Based Multi-levels Optimization Design of Structures, IEIT Journal of Adaptive & Dynamic Computing, 2011(4), Oct 2011, pp:1-8. DOI=10.5813/www.ieit-web.org/IJADC/2011. 4.1

[6] M.P.Vani, Computer Aided Interactive Process of Teaching Statistics Methodology – III Evaluation Questionnaire for LearnersThrough statistical display using Bar chart, IEIT Journal of Adaptive & Dynamic Computing, 2011(4), Oct 2011, pp:9-14. DOI=10.5813/www.ieit-web.org/IJADC/20114.2

[7] Lo. Yu-Lung, Jen-Fa Huang and Po-Hsun Sung et al: Intensity variation effects in fiber Bragg grating sensors scanned by a tunable filter, Meas.Sci.Technol.2000, pp.1456-1462.

[8] C. S. Quang, W. J. Lee. "A TSK-Type Neuro-Fuzzy network approach to system modeling problems," IEEE Trans. On Sys. Man and   Cyberntic, Vol. 35, No. 4, 2005.

[9] V. Topalov, G. L. Cascella, V. Giordano, F. Cupertino, O. Kaynak, "Sliding mode Neuro-Adaptive control of electrical drives," IEEE Trans. Indust. Electron., V. 54, No. 1, pp. 671-679, 2007.

[10] Seda Postalcioglu,Yasar Becerikli ."Wavelet Networks for Nonlinear System Modeling", Neural Comput & Applic, Vol. 16, p.p 433-441, 2007.